Spectral characteristics of arc plasma during laser-arc double-sided welding for aluminum alloy

Kezhao Zhang (张可召), Zhenglong Lei (雷正龙)*, Xianglong Wang (王祥龙), Yanbin Chen (陈彦宾), and Yaobang Zhao (赵耀邦)

State Key Laboratory of Advanced Welding and Joining, Harbin Institute of Technology, Harbin 150001, China

**Corresponding author: leizhenglong@hit.edu.cn*

Received January 24, 2015; accepted April 8, 2015; posted online May 11, 2015

In laser-arc double-sided welding, the spectral characteristics of the arc plasma are calculated and analyzed by spectroscopic diagnosis. The results show that, compared with conventional tungsten inert gas (TIG) welding, the introduction of a laser changes the physical characteristics of the arc plasma regardless of whether laser plasma penetration takes place, and that the influence of the laser mainly affects the near-anode region of the arc. When the laser power is relatively low, the arc column tends to compress, and the arc spectral characteristics show no significant difference. When the arc root constricts, compared with pure TIG arc, the electron density increases by ~2.7 times and the electron temperature decreases by ~3000 K. When the arc column expands, the intensities of spectral lines of both the metal and Ar atoms are the strongest. But it is also observed that the electron density reduces, whereas there is no obvious decrease of electron temperature.

OCIS codes: 140.3390, 350.3390, 300.6170.

doi: 10.3788/COL201513.061403.

In recent years, laser-arc hybrid welding has been intensively investigated in the field of laser welding[1]. It is widely acknowledged that the arc can be attracted and compressed by the laser in the hybrid process, thereby increasing the penetration depth and welding velocity, and making hybrid welding a more efficient method than the sum of its two heat sources[2–4]. At present, the research of laser-arc hybrid welding mainly focuses on the interaction between the laser and the arc plasma, as well as the heat flow and mass transport processes[5–8]. But the research focus is the conventional laser-arc hybrid welding, namely single-side hybrid welding. During single-side hybrid welding process, however, it is hard to individually describe the characteristics of the laser and the arc due to their overlapping melting pools and plasmas, so the research concerning the mechanism mainly pays attention to the image of hybrid arc plasma, the varieties of current and voltage, and so on[2,9]. And the component and the density of hybrid arc plasma have not been analyzed owing to the nonaxial symmetry of arc. Moreover, the spectrum characterization of laser plasma only concentrated on laser-induced air plasma and the generation of terahertz waves[10,11]. Recently, Chen proposed an improved laser-arc hybrid welding method called laser-arc double-sided welding (LADSW). Compared with the conventional laser welding or tungsten inert gas (TIG) arc welding of Aluminum alloys, the LADSW can stabilize the welding process significantly, improve the weld surface appearance, greatly reduce or even eliminate the welding defects, as well as enhance the energy utilization and welding adaptability. In addition, an apparatus for characterizing the interaction between laser, arc, and laser-induced plasma was set up in the LADSW, and the effects of the laser-induced plasma on the arc plasma were studied[12]. In the previous works, as the laser power was increased, three typical arc behaviors were observed: (i) arc column compression due to laser keyhole preheating [Fig. 1(b)], (ii) arc root constriction due to a small amount of laser plasma penetration [Fig. 1(c)], and (iii) arc column expansion due to considerable laser plasma penetration in LADSW [Fig. 1(d)][13,14]. To the best of our knowledge, no research investigating the forming cause of three different arc shapes, and the arc spectral characteristics in correlation with the variation of electron density and temperature have been reported to date. In this work, in order to further understand the hybrid welding phenomena and the underlying welding mechanisms, the spectra of the arc plasma were analyzed during the LADSW process with a spectrometer. The variations of electron density and temperature of the welding arc with respect to different laser powers are obtained. And the physical characteristics of the arc plasma under the influence of the laser are revealed, which further enhance the theory underlying laser-arc hybrid welding.

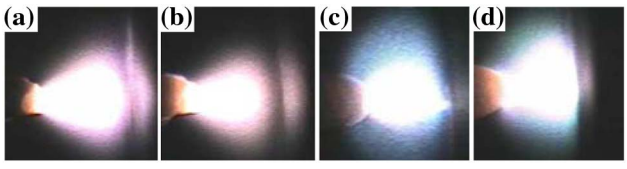

Fig. 1. Typical arc shapes in LADSW ($I = 60$ A) under different laser power configurations: (a) Pure TIG arc, (b) arc column compression, (c) arc root constriction, and (d) arc column expansion shapes occur under $P = 0$, 1.6, 2.0, and 2.8 kW, respectively.

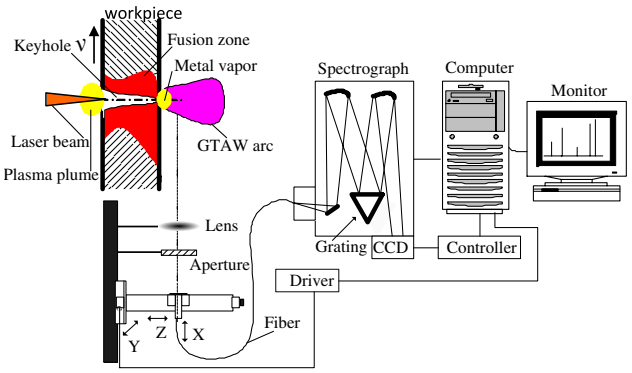

Fig. 2. Schematic diagram of the welding experiment and arc spectral collecting system.

The arc plasma spectra of the LADSW are measured by a SP556 spectrometer, as shown in Fig. 2. The heat sources of the LADSW consist of a CO_2 (Rofin–Sinar) and an inverter argon WX300 arc welding system (Panasonic). Bead-on-plate welding was performed on 4 mm thick 5A06 aluminium alloy plate. The material composition is provided in Table 1. During the process, CO_2 laser beam and TIG torch were vertically located on the opposite sides of a workpiece, and kept immobile, while the workpiece was moved by a vertical worktable. The focal length of the lens in the experiments is 200 mm, the distance between arc and lens is 300 mm. According to the principle of imaging, an amplified inverted real image will emerge at the rear of the lens by 600 mm in the proportion of 1:2. The light-pass slit can obtain the spatial resolution by the selectivity of the radiation light in the whole arc space, and the width of the incident slit is 0.05 mm, the optical fiber probe can couple the arc radiation light into the spectrometer. A 300 g/mm (blaze = 500) grating with a resolution of 0.156 nm was used and the wavelength range covered approximately 160 nm. A thermoelectrically cooled CCD, model TE/CCD-1100PF manufactured by Princeton Instrument with high thermal stability was used as detector. The working temperature of the CCD was −30°C, the exposure time is 0.5 s. When the TIG arc welding is stable, we assume that the arc remains unchanged, and click the settings to start the measurement in WinSpec32 software, the acquisition time is consistent with the exposure time, that is 0.5 s. The signals were transmitted to an ST133 controller manufactured by Princeton Instrument, where they were processed and displayed by a WinSpec32 software on a computer. The spectra of arc plasma were acquired on the axis of arc plasma, and the fiber was vertically moved along the z-direction on the image plane during the scanning. Spectral lines were identified by comparison to the wavelengths listed in the referenced data of NIST Atomic Spectra Database. In order to ensure the validity, the work is carried out 5× in the same parameters, so the intensity, electron temperature, and electron density are taken considering the average value of five calculation results.

In optically thin plasma, the intensity of a given spectral line I_{mn}, which is induced by the electron transition from Level m to Level n, can be described by

$$I_{\mathrm{mn}} = N_{\mathrm{m}} A_{\mathrm{mn}} \mathrm{h}\upsilon_{\mathrm{mn}}, \tag{1}$$

where N_{m} is the electron density of the upper level, h is Planck's constant, A_{mn} is the transition probability, and v_{mn} is the frequency of the spectral line from Level m to Level n[15,16].

Since the TIG arc is axisymmetric in LADSW, the welding plasma is assumed to be in local thermal equilibrium[15]. The Boltzmann distribution and the Saha equation are applied to determine the plasma temperature. As we reported previously[13], the electron temperature of the arc (T) can be calculated by the Saha–Boltzmann equation

$$\ln\left(\frac{I_{\mathrm{pq}}\lambda_{\mathrm{pq}}A_{\mathrm{mn}}g_{\mathrm{mn}}}{I_{\mathrm{mn}}\lambda_{\mathrm{mn}}A_{\mathrm{pq}}g_{\mathrm{pq}}}\right) = -\frac{1}{KT}(E_{\mathrm{p}} - E_{\mathrm{m}} + E_{\mathrm{z}\infty} - \Delta E_{\mathrm{zI}}) + \ln\left(2\frac{(2\pi \mathrm{m}kT)^{3/2}}{N_{\mathrm{e}}\mathrm{h}^3}\right), \tag{2}$$

where λ_{mn} is the wavelength of the spectral line from Level m to Level n, g_{mn} is the statistical weight from Level m to Level n, E_{m} is the excitation energy of the upper level, $E_{z\infty}$ is the ionization energy of Species z for isolated systems, E_{zI} is the correction of this quantity for interactions in the plasma, m is the electron mass, k is Boltzmann's constant (1.381×10^{-23} J · K^{-1}), and T is the electron temperature. Additionally, we noted[13] that the electron density of the arc (N_{e}) can be determined by means of the Starks broadening effect

$$N_{\mathrm{e}} = \frac{\Delta\lambda_{\frac{1}{2}}^{S}}{2\omega} \times 10^{16}, \tag{3}$$

where $\Delta\lambda_{\frac{1}{2}}^{S}$ is the full-width at half-maximum (FWHM), and ω is the broadening factor of electron collision. The FWHM of Ar I (763.511 nm) was obtained by Lorentzian fitting, and the broadening factor ω was obtained from Ref. [17].

During the LADSW process, it is found that the introduction of the laser changes the physical characteristics of the arc plasma whether laser plasma penetration occurs or not. Figure 3 presents a comparison of the arc spectra

Table 1. Chemical Composition of 5A06 Al Alloy

Element	Mg	Mn	Si	Fe	Zn	Cu	Ti	Al
Content (wt. %)	5.8–6.8	0.5–0.8	0.4	0.4	0.2	0.10	0.02–0.10	Balance

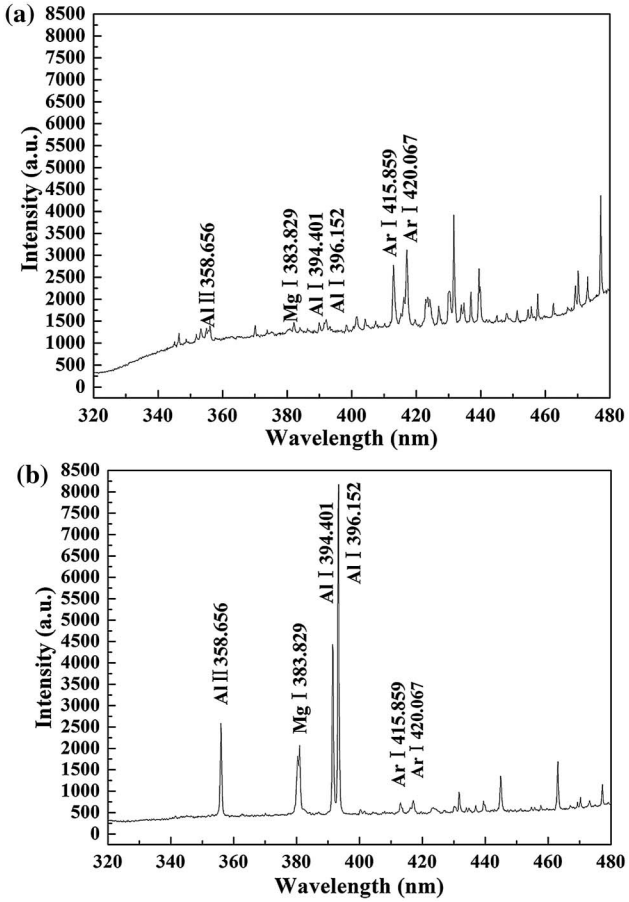

Fig. 3. Arc spectral characteristics of (a) conventional TIG arc, and (b) LADSW ($I = 60$ A, $v = 1$ m/min, and $P = 2.0$ kW).

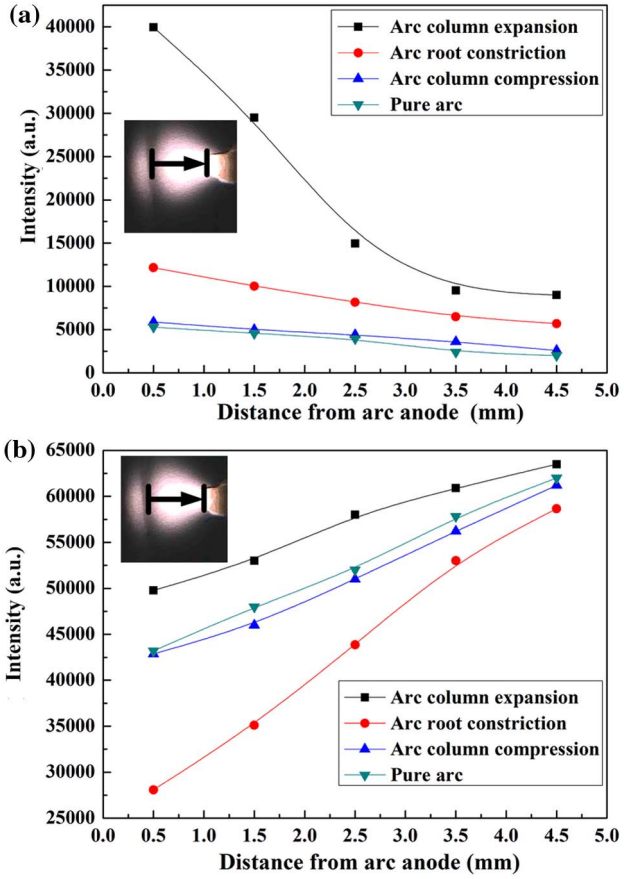

Fig. 4. Intensities of (a) Al I 396.152 and (b) Ar I 763.511 of the arc plasma on the arc axes with typical arc images.

measured during conventional TIG welding [Fig. 3(a)], and LADSW [Fig. 3(b)] in the middle of the arc axes within the wavelength range of 320–480 nm. It is found that the intensities of the spectral lines of Al and Mg atoms are much stronger in LADSW, while those of Ar atoms are weaker. In TIG welding, the intensity distribution is just the opposite.

In fact, the laser has a gradual effect on the arc spectra intensities in arc space in the LADSW process. According to the spectral intensity curve acquired from 320–480 and 640–800 nm[13], the spectrum lines of Al I (396.152 nm) and Ar I (763.511 nm) in which the intensity is the largest were chosen to compare the changes of arc plasma in TIG welding with that in LADSW. Figure 4 shows the intensity distribution of Al I 396.152 and Ar I 763.511 along the arc axes with respect to arc shape. Generally speaking, the arc shapes differ more greatly close to the anode, and differ less near the cathode, which indicates that the influence of laser is mainly restricted to the near-anode region. Meanwhile, in the same arc position, the intensities of both spectral lines are the strongest in the arc column expansion mode. It is found the intensities of Al I 396.152 are weaker in the arc root constriction mode, and are weakest (and nearly identical) in the pure arc and the arc column compression modes. As for the Ar I 763.511, the intensities are weak in the pure arc and the arc column compression modes, while the intensity is weakest in the arc root constriction mode.

In order to further analyze the effects of the laser on the arc spectral intensities in the different arc shapes, the variation of the spectral line intensities of metal atoms (Al I 396.152) and Ar atoms (Ar I 763.511) was studied with respect to the laser power. These results are shown in Fig. 5. During the LADSW process, the intensities of the spectral lines for the metal atoms increase monotonically with increasing laser power, while the intensity of Ar I 763.511 decreases first and then increases. At relatively low power, the laser does not penetrate through the workpiece, but compression of the arc column is still observed in the LTDSW. Since only a small fraction of Al atoms are vaporized from the melting pool, the arc plasma consists mainly of Ar atoms. Because of this the intensity of Ar I 763.511 can be as high as 48000, whereas the intensity of Al I 396.152 is only about 6000. When the laser power exceeds a critical value, namely, when the laser plasma just penetrates through the workpiece, the arc root will be constricted. As a result, some of the laser-induced metal plasma, full of Al atoms, is ejected from the side of TIG arc. Accordingly, the intensity of Al I 396.152 is larger. The increase of metal atoms therefore lowers the

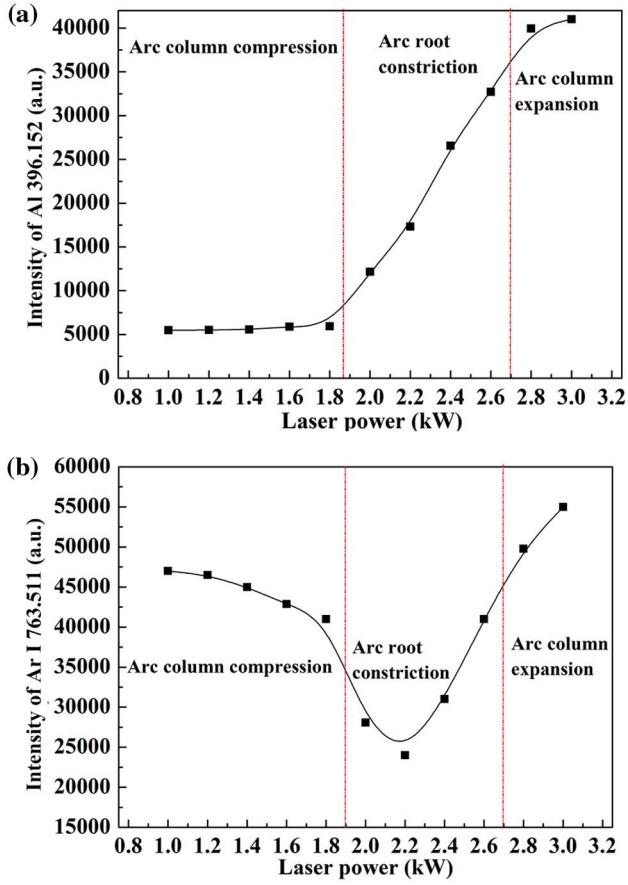

Fig. 5. Effect of laser power ($I = 60$ A and $v = 1$ m/min) on the spectral intensities of (a) Al I 396.152 and (b) Ar I 763.511.

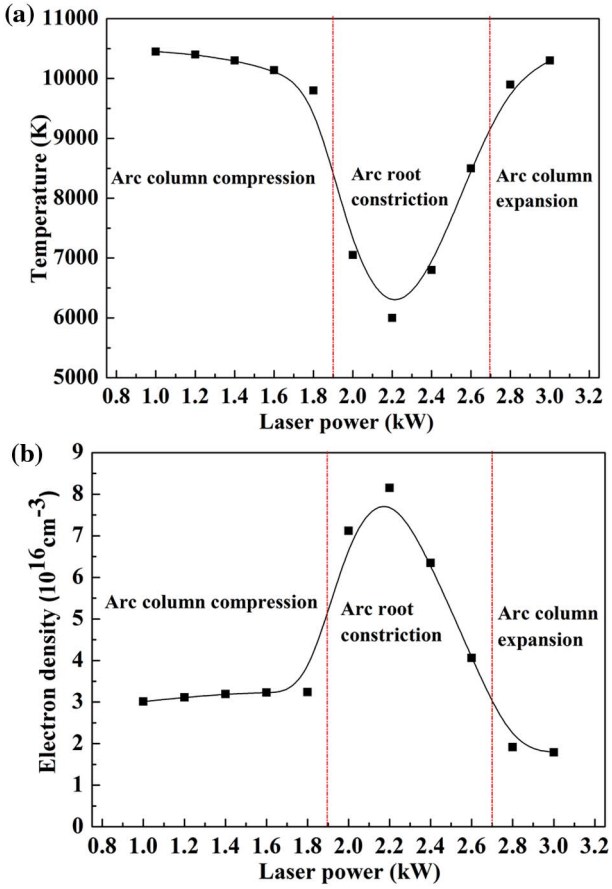

Fig. 6. Effect of laser power ($I = 60$ A and $v = 1$ m/min) on (a) electron temperature and (b) electron density during LADSW.

intensity of Ar I 763.511. This first critical value of laser plasma penetration can be clearly seen at 1.9 kW in Figs. 5(a) and 5(b) and is indicated by the dashed vertical red lines. If laser power continues to increase, the expansion of the welding arc can be observed and the content of Al atoms in the arc will keep on increasing, resulting in an intensity of 40000 or higher. At this point, the laser works directly on the arc. It is likely that the welding arc absorbs the laser energy by inverse bremsstrahlung, leading to more excited-state Ar atoms. Therefore, the intensity of Ar I 763.511 has considerably increased[18], as shown in Fig. 5(b).

Since the introduction of the laser changes the spectral characteristics of the arc plasma in LADSW, it is natural that the electron temperature and density in the arc plasma are also different than in conventional TIG arc. Figure 6 shows the variation of the electron temperature and density at the axial position of 0.5 mm above the anode with respect to laser power in LADSW. It is observed that the electron temperature and density change in opposite directions, as seen in Fig. 6. When the laser power is relatively low (i.e., in the arc column compression mode), the electron temperature and density of arc plasma change only subtly with increasing laser power. Their values are maintained close to about 10000 K and 3×10^{16} cm^{-3}, respectively. When the laser power exceeds a threshold (i.e., in the arc root constriction mode), the electron temperature and density of the arc plasma change dramatically. The electron temperature falls to around 6000–8500 K, while the electron density rapidly increases by a factor of 2.7 compared with the pure TIG arc, up to a maximum of 8.1×10^{16} cm^{-3}. In the arc column expansion mode, the electron temperature rises back up to approximately 10000 K, which is comparable to the stage when the arc column converges. On the other hand, the electron density decreases to a minimum value of 1.8×10^{16} cm^{-3}. It follows that the electron temperature and density of the arc plasma are closely related to the arc shape. A constricted arc will always results in higher densities of electrons and current, while those of the expanded arc behave in the opposite manner.

In conclusion, in LADSW the introduction of a laser changes the physical characteristics of the arc plasma irrespective of the occurrence of laser plasma penetration. The arc column tends to compress when the laser power is relatively low. With no laser-induced metal plasma entering the welding arc, there are no significant changes observed in the arc spectral characteristics. In the arc root constriction mode, a little laser-induced metal plasma accumulates at the arc root, which leads to an increase in the intensities of the metal atom spectral lines and a

decrease in the Ar atom spectral lines. During this arc root constriction, the electron density increases by 2.7 times compared to pure TIG arc at the arc root, while the electron temperature decreases by ~3000 K. The arc tends to expand when considerable laser-induced plasma enters the arc. In this case, the intensities of spectral lines for metal and Ar atoms simultaneously reach their maxima. In this high laser power regime, the electron density decreases from 3×10^{16} cm^{-3} (pure TIG arc) to 1.8×10^{16} cm^{-3}, whereas the electron temperature changes very little as compared to that of the pure TIG arc.

This work was supported by the National Natural Science Foundation (Grant No. 51105105) and the Fundamental Research Funds for the Central Universities (Grant No. HIT NSRIF 201137).

References

1. B. Ribic, T. A. Palmer, and T. DebRoy, Int. Mater. Rev. **4**, 54 (2009).
2. Y. B. Chen, Z. L. Lei, L. Q. Li, and L. Wu, Sci. Technol. Weld. Join. **4**, 11 (2006).
3. P. T. Swanson, C. J. Page, and E. Read, Sci. Technol. Weld. Join. **2**, 12 (2007).
4. L. E. Guen, R. Fabbro, and M. Carin, Opt. Laser Technol. **7**, 43 (2011).
5. B. Ribic, R. Rai, and T. DebRoy, Sci. Technol. Weld. Join. **8**, 13 (2008).
6. Y. T. Cho, W. I. Cho, and S. J. Na, Opt. Laser Technol. **3**, 43 (2011).
7. B. Ribic, R. Rai, and T. DebRoy, Sci. Technol. Weld. Join. **8**, 13 (2008).
8. D. W. Cho, W. I. Cho, and S. J. Na, J. Manuf. Process. **1**, 16 (2014).
9. R. Huang, L. Liu, and F. Zhang, Chin. Opt. Lett. **6**, 356 (2008).
10. J. Zhao, L. Zhang, Y. Luo, T. Wu, C. Zhang, and Y. Zhao, Chin. Opt. Lett. **12**, 083201 (2014).
11. S. Yi, B. Mu, X. Wang, J. Zhu, L. Jiang, Z. Wang, and P. He, Chin. Opt. Lett. **12**, 013401 (2014).
12. Y. B. Chen, Y. G. Miao, and L. Q. Li, Sci. Technol. Weld. Join. **5**, 13 (2008).
13. Y. B. Chen, Y. B. Zhao, Z. L. Lei, and L. Q. Li, Sci. Technol. Weld. Join. **1**, 17 (2012).
14. Y. B. Zhao, Z. L. Lei, and L. Q. Li, J. Mech. Eng. **4**, 49 (2013).
15. H. R. Griem, *Principles of Plasma Spectroscopy* (Cambridge University, 2005).
16. C. Aragon and J. A. Aguilera, Spectrochim. Acta B **9**, 63 (2008).
17. N. Konjevic, A. Lesage, J. R. Fuhr, and W. L. Wiese, J. Phys. Chem. Ref. Data **31**, 2 (2002).
18. S. K. Wu, "Investigation on laser-arc interaction and novel laser-TIG arc hybrid welding processes," Ph.D. thesis (Beijing University of Technology, 2010).